

## MIMETIC FINITE DIFFERENCES FOR ELLIPTIC PROBLEMS

FRANCO BREZZI<sup>1</sup>, ANNALISA BUFFA<sup>2</sup> AND KONSTANTIN LIPNIKOV<sup>3</sup>

**Abstract.** We developed a mimetic finite difference method for solving elliptic equations with tensor coefficients on polyhedral meshes. The first-order convergence estimates in a mesh-dependent  $H^1$  norm are derived.

**Mathematics Subject Classification.** 65N06, 65N12, 65N15, 65N30.

Received December 5, 2007. Revised July 21, 2008.

Published online December 5, 2008.

### 1. INTRODUCTION

For numerical solution of partial differential equations, polyhedral meshes can provide several advantages. For instance, a polyhedral mesh has fewer mesh faces than a tetrahedral one with the same mesh resolution, which increases performance of linear solvers. Moreover in computational fluid dynamics it is often desirable to have element faces perpendicular to the flow. A polyhedral element with many faces increases the probability of having such faces. As mentioned in [11], this results in a smaller numerical diffusion and a more accurate solution.

More generally, polyhedral meshes have enormous flexibility in representing complex geometries. The adaptive mesh refinement technique, which is used to optimize available computational resources and is an essential part of modern multi-physics codes, results in polyhedral meshes with degenerate elements. Non-matching meshes can also be seen as polyhedral meshes with degenerate elements. Another technique for modeling complex porous media structures, such as pinch-outs and faults, is to collapse edges of a hexahedral element to points which results in polyhedral elements with strongly curved faces [12].

In this article, we use the mimetic finite difference (MFD) discretization technique which has been designed to work on general polyhedral meshes without any special treatment of degenerate elements. From each polyhedron, the MFD method requires only boundary data such as areas, barycenters and normals to faces, which simplifies its usage for elements with irregular shapes.

The MFD method produces a compatible discretization where discrete analogs of differential operators retain their important properties, so that conservation laws, solution symmetries, and the fundamental identities of vector and tensor calculus do hold for discrete systems. For example, the discrete divergence and gradient operators are negatively adjoint with respect to inner products in discrete spaces. This property has a number of useful consequences. For diffusion problems, it results in symmetric discretizations and simplifies their

---

*Keywords and phrases.* Finite differences, polyhedral meshes, diffusion equation, error estimates.

<sup>1</sup> Istituto Universitario di Studi Superiori, Pavia, Italy. [brezzi@imati.cnr.it](mailto:brezzi@imati.cnr.it)

<sup>2</sup> Istituto di Matematica Applicata e Tecnologie Informatiche, Pavia, Italy. [annalisa@imati.cnr.it](mailto:annalisa@imati.cnr.it)

<sup>3</sup> Los Alamos National Laboratory, Theoretical Division, MS B284, Los Alamos, NM, 87545, USA. [lipnikov@lanl.gov](mailto:lipnikov@lanl.gov)

convergence analysis [4]. For compressible flow simulations, it helps to build discretizations that preserve total momentum and energy, see *e.g.* [13].

In articles [4–7], we developed new analysis of mimetic discretization methods for solving elliptic equations on polyhedral meshes. In the case of polyhedral meshes, these discretizations use one flux unknown per mesh face and one scalar unknown (pressure, temperature, *etc.*) per mesh element. In the case of generalized polyhedral meshes, three flux unknowns per curved faces are required to build a mimetic method [6,7]. For simplicial meshes, the family of MFD methods contains the mixed finite element method with the lower-order Raviart-Thomas elements [14]. In this article, we develop and analyze new nodal mimetic methods.

As in [5,7], here we build again *a family* of discretization methods which is reduced to the standard  $P_1$  finite element method [9] in the case of simplicial meshes. Under weak assumptions on the mesh regularity, each method in the family provides the first-order convergence rate in the mesh dependent energy norm.

There are a few advantages of using of a polyhedral mesh rather than an equivalent tetrahedral mesh with the same nodes. First, building of a conformal tetrahedral partition requires analysis of geometry which comes with additional computational overhead, especially for moving mesh methods. Indeed, for a given partition of polyhedron's faces into triangles, a tetrahedral partition using only the polyhedron vertices may not exist! Second, there are two ways to break a quadrilateral element into two triangles. The question of choosing the better partition is transformed to finding a proper member in a family of MFD methods, which provides a new numerical and analytical tool for future research. Third, a symmetric breaking may be required for special problems and it can be hardly done without using additional points. In shock calculations, where the nodal discretization of an elliptic equation is used to add a numerical viscosity to the system [8], a non-symmetric breaking may quickly destroy solution symmetry.

Recently, more general frameworks for mimetic discretizations have been developed using algebraic topology and cochain approximations of differential forms [1,3]. The key concept of [1] is a natural inner product on cochains which induces a combinatorial Hodge theory on the cochain complex. This article provides the constructive method for building one of the inner products.

The article outline is as follows. In Section 2, we define the elliptic problem. In Section 3, a class of admissible polyhedral meshes is described. In Section 4, the discrete operators are introduced. In Section 5, the discrete MFD method is formulated. In Section 6, first-order error estimates in energy norm are proved. The theoretical results are verified with numerical experiments in Section 7.

## 2. THE CONTINUOUS PROBLEM

Let  $\Omega \subset \mathbb{R}^3$  be a bounded Lipschitz polyhedron,  $g \in L^2(\Omega)$  and  $\mathbb{K}$  be a regular symmetric positive definite tensor  $\mathbb{K} \in (W^{1,\infty}(\Omega))^{3 \times 3}$ . We look for the solution  $u \in H_0^1(\Omega)$  of the boundary value problem

$$-\operatorname{div} \mathbb{K} \mathbf{grad} u = g \quad \text{in } \Omega. \quad (2.1)$$

Extension to other boundary conditions is straightforward. This problem admits the variational formulation: Find  $u \in H_0^1(\Omega)$  such that

$$\int_{\Omega} \mathbb{K} \mathbf{grad} u \cdot \mathbf{grad} v \, dx = \int_{\Omega} g v \, dx \quad \forall v \in H_0^1(\Omega), \quad (2.2)$$

and we will discretize the problem in this form. For further use, we set:

$$(u, v) := \int_{\Omega} \mathbb{K} \mathbf{grad} u \cdot \mathbf{grad} v \, dx. \quad (2.3)$$

In what follows, we assume that there exist two constants  $\kappa_\star$  and  $\kappa^\star$  such that:

$$\kappa_\star \mathbf{v}^T \mathbf{v} \leq \mathbf{v}^T \mathbb{K}(\mathbf{x}) \mathbf{v} \leq \kappa^\star \mathbf{v}^T \mathbf{v} \quad \forall \mathbf{v} \in \mathbb{R}^3, \mathbf{x} \in \Omega. \tag{2.4}$$

All constants in the estimates proposed in this paper will depend upon  $\kappa_\star$  and  $\kappa^\star$ .

Throughout this paper, we shall use  $\|\cdot\|_{n,D}$  and  $|\cdot|_{n,D}$  to denote the norm and semi-norm, respectively, on the Hilbert space  $H^n(D)$ , where  $D \subset \Omega$ . If  $D = \Omega$ , subscript  $D$  may be omitted. Finally, for further use, we set  $\mathcal{H}^1(\Omega) = H_0^1(\Omega) \cap C^0(\overline{\Omega})$ .

### 3. THE DECOMPOSITION

#### 3.1. Notation

We assume that on  $\Omega$  we are given a sequence  $\{\mathcal{T}_h\}_h$  of regular polyhedral meshes  $\mathcal{T}_h$  in a sense of assumption **(HG)**. This means that for each  $\mathcal{T}_h$  the domain  $\Omega$  is split into  $n_P$  polyhedra  $P_1, \dots, P_{n_P}$ , with  $n_V$  vertices  $V_1, V_2, \dots, V_{n_V}$ .

For every geometric object  $Q$  (edge, face, polyhedron, *etc.*), we will denote its *diameter* by  $h_Q$ . Moreover, for every decomposition  $\mathcal{T}_h$  we set

$$|h|_{\mathcal{T}_h} := \max_{P \in \mathcal{T}_h} h_P. \tag{3.1}$$

Most of the times, the subscript will be omitted, and we shall simply write it as  $|h|$ . We denote by  $\mathcal{V}(\mathcal{T}_h)$ ,  $\mathcal{L}(\mathcal{T}_h)$  and  $\mathcal{F}(\mathcal{T}_h)$  the set of vertices, edges and faces of the decomposition  $\mathcal{T}_h$ . The corresponding sets of internal vertices, edges and faces are denoted by  $\mathcal{V}_0(\mathcal{T}_h)$ ,  $\mathcal{L}_0(\mathcal{T}_h)$  and  $\mathcal{F}_0(\mathcal{T}_h)$ , respectively.

#### 3.2. Assumptions on the decompositions

As we shall see, the properties of the decompositions that are needed in our approach are very weak, meaning that we are allowed a great freedom in the choice of the shape of the polyhedral elements.

However, to make the description simpler, we will make some assumptions that are *stronger than necessary*. It will nevertheless be clear in the following discussion that more general situations can be tackled.

We assume that there exist two positive real numbers  $N_s$  and  $\rho_s$  (the same for all the sequence) such that for every decomposition  $\mathcal{T}_h$  in the sequence we have:

**(HG)** (*Regular polyhedral decomposition  $\mathcal{T}_h$* ): There exists a *compatible* sub-decomposition  $\mathcal{S}_h$  into *shape-regular* tetrahedra, such that

- Every polyhedron  $P \in \mathcal{T}_h$  admits a decomposition  $\mathcal{S}_{h|P}$  made of less than  $N_s$  tetrahedra;
- The shape-regularity of the tetrahedra  $K \in \mathcal{S}_h$  is defined as follows [9]: the ratio between the radius  $r_K$  of the inscribed sphere and the diameter  $h_K$  is bounded from below by constant  $\rho_s$ :

$$\frac{r_K}{h_K} \geq \rho_s > 0. \tag{3.2}$$

It is important to point out, from the very beginning, that there is no need, in practice, to build the decomposition  $\mathcal{S}_h$ . We are only assuming that *it does exist* (or, better, that *it could be built*). In practice, we are essentially avoiding sequences of decompositions in which there are polyhedra that are, asymptotically, more and more hourglass-shaped or having thinner and thinner tails (see Fig. 1): a choice which is hardly conceivable by any user of our numerical method.

#### 3.3. Consequences of the assumption **(HG)**

The above requirements have several consequences, that can be easily verified. Among them we underline the following ones which will be used later.

**(C1)**: There exist integer numbers  $N_f$ ,  $N_e$  and  $N_v$  (depending only on  $N_s$ ) such that every polyhedron in every decomposition has less than  $N_f$  faces, less than  $N_e$  edges, and less than  $N_v$  vertices.

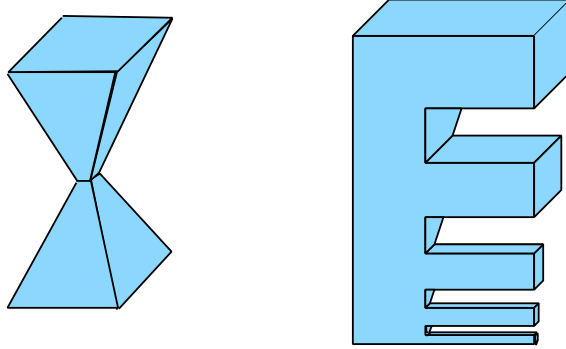


FIGURE 1. Hourglass (left) and thin-tailed (right) polyhedra.

**(C2):** There exists a positive number  $\sigma_s$  (depending only on  $N_s$  and  $\rho_s$ ) such that

$$h_e \geq \sigma_s h_f \geq \sigma_s^2 h_P, \quad (3.3)$$

whenever  $e$  is an edge of  $f$  and  $f$  is a face of  $P$ .

**(C3):** For every face  $f$ , there exists a decomposition of  $f$  in a finite number ( $\leq N_s$ ) of *regular shaped* triangles, meaning that there exists a positive constant  $\sigma_\phi$  depending only on  $\rho_s$  such that for every triangle  $T$  we have

$$r_T \geq \sigma_\phi h_T, \quad (3.4)$$

where  $r_T$  is the radius of the inscribed circle and  $h_T$  is the diameter of  $T$ .

**(C4):** There exists a constant  $\gamma_a$ , depending only on  $N_s$  and  $\rho_s$  such that for every polyhedron  $P$  and for every face  $f$  of  $P$  we have the *Agmon inequality*

$$\int_f \varphi^2 dS \leq \gamma_a \left( h_P^{-1} \|\varphi\|_{L^2(P)}^2 + h_P \|\mathbf{grad} \varphi\|_{L^2(P)}^2 \right). \quad (3.5)$$

## 4. THE DISCRETE OPERATORS

### 4.1. The discrete unknowns

We consider now the set  $\mathcal{V}(\mathcal{T}_h)$  of *vertices* in  $\mathcal{T}_h$  and the set  $\mathcal{N}$  of *nodal values* on  $\mathcal{V}(\mathcal{T}_h)$ , that is the mappings from  $\mathcal{V}(\mathcal{T}_h)$  into  $\mathbb{R}$ . We will also consider the subset  $\mathcal{N}_0$  of the nodal unknowns that vanish at the vertices  $V \in \partial\Omega$ , that is

$$\mathcal{N}_0 := \{u \in \mathcal{N} \text{ such that } u(V) = 0 \quad \forall V \in \mathcal{V}(\mathcal{T}_h), V \in \partial\Omega\}. \quad (4.1)$$

In a similar way we can consider the set  $\mathcal{E}$  of *edge unknowns* as the mappings from the set of all *oriented edges* of  $\mathcal{T}_h$  to  $\mathbb{R}$ .

### 4.2. Restrictions of unknowns

When considering the restrictions of *unknowns* (or, more generally, *mappings*) to a given geometrical object  $Q$  we would generally use the subscript  $|_Q$  or simply  $Q$ . For instance, both  $\mathcal{N}|_Q$  and  $\mathcal{N}_Q$  will denote the restriction of  $\mathcal{N}$  to the nodes belonging to  $Q$ .

### 4.3. The $\mathcal{GRAD}$ operator

It will often be convenient to consider the  $\mathcal{GRAD}$  operator, defined from the set of nodal unknowns  $\mathcal{N}$  to the set of edge unknowns  $\mathcal{E}$  as follows: for each element  $u \in \mathcal{N}$  and for each edge  $e$  with vertices  $(V_1, V_2)$ , oriented

from  $V_1$  to  $V_2$ ,

$$(\mathcal{GRAD} u)|_e = u(V_2) - u(V_1). \tag{4.2}$$

Sometimes, it will be convenient to consider the application of the  $\mathcal{GRAD}$  operator to a subset of  $\mathcal{N}$ . Given a polyhedron  $P \in \mathcal{T}_h$ , the operator  $\mathcal{GRAD}_P$  (defined exactly as in (4.2)) maps  $\mathcal{N}_P$  into  $\mathcal{E}_P$ . It is obvious that  $\mathcal{GRAD}_P$  is a restriction of  $\mathcal{GRAD}$ , and it will also be denoted by  $\mathcal{GRAD}$  when no confusion can occur. Finally we set

$$\mathcal{E}_0 = \{\tau \in \mathcal{E} : \tau(e) = 0 \quad \forall e \in \mathcal{L}(\mathcal{T}_h), e \in \partial\Omega\}.$$

It is easy to see that  $\mathcal{GRAD}$  maps also  $\mathcal{N}_0 \rightarrow \mathcal{E}_0$ .

If  $u_h \in \mathcal{N}_0$  is taken as an approximation of the scalar function  $u$  that solves (2.2), then  $\mathcal{GRAD} u_h$  is an element of  $\mathcal{E}_0$  and the operator  $\mathcal{GRAD}$  is related to the operator **grad**.

#### 4.4. The norm in $\mathcal{N}_0$

In the space of our unknowns  $\mathcal{N}_0$ , we can now introduce the following norm:

$$\|v_h\|^2 := \sum_{P \in \mathcal{T}_h} \|v_h\|_P^2 := \sum_{P \in \mathcal{T}_h} h_P \sum_{e \in \partial P} \left| (\mathcal{GRAD}_P v_h)|_e \right|^2. \tag{4.3}$$

Note that, essentially from (3.3), the norm in the above (4.3) is equivalent to

$$\|v_h\|^2 \simeq \sum_{P \in \mathcal{T}_h} h_P^3 \sum_{e \in \partial P} \left| \frac{(\mathcal{GRAD}_P v_h)|_e}{|h_e|} \right|^2, \tag{4.4}$$

mimicking the  $H_0^1(\Omega)$ -norm.

#### 4.5. The interpolation and reconstruction operators

We shall now define the natural interpolation operators  $\Pi_{\mathcal{N}}$  from  $\mathcal{H}^1(\Omega)$  to the discrete space  $\mathcal{N}$ . For each  $u$  in  $\mathcal{H}^1(\Omega)$  we define  $\Pi_{\mathcal{N}}u \in \mathcal{N}$  by

$$(\Pi_{\mathcal{N}}u)|_V = u(V) \quad \forall V \in \mathcal{V}(\mathcal{T}_h). \tag{4.5}$$

Let us consider the problem of finding continuous right inverses of the interpolation operator  $\Pi_{\mathcal{N}}$ . We shall see in Appendix A that, under assumption **(HG)** on the decomposition  $\mathcal{T}_h$ , there exists a constant  $\gamma$  depending solely on  $N_s$  and  $\rho_s$ , and a linear operator  $v_h \rightarrow R_{\mathcal{N}}v_h$  from  $\mathcal{N}$  into  $\mathcal{H}^1(\Omega)$  with the following properties:

- For every  $v_h \in \mathcal{N}$ ,

$$\Pi_{\mathcal{N}}R_{\mathcal{N}}v_h = v_h. \tag{4.6}$$

- For every  $v_h \in \mathcal{N}_0$  and for every polyhedron  $P \in \mathcal{T}_h$ ,

$$|R_{\mathcal{N}}v_h|_{1,P}^2 \leq \gamma \|v_h\|_P^2. \tag{4.7}$$

- For every  $v_h \in \mathcal{N}_0$ , for every polyhedron  $P \in \mathcal{T}_h$  and for every vertex  $V \in P$ ,

$$\|R_{\mathcal{N}}v_h - v_h(V)\|_{0,P}^2 \leq \gamma h_P^2 \|v_h\|_P^2. \tag{4.8}$$

The existence of such a reconstruction is the only reason why we ask for the assumption **(HG)** to hold. It is clear then that the assumption **(HG)** is abundant. We have chosen it only to allow a *simple* construction (see App. A), and in particular one that does not require too much functional analysis.

For further use, we note that from (4.7), (4.8) and (3.5), we immediately have the following result:

- For every  $v_h \in \mathcal{N}_0$ , for every polyhedron  $P \in \mathcal{T}_h$ , for every face  $f \in \partial P$ , and for every vertex  $V \in f$

$$\|R_{\mathcal{N}}v_h - v_h(V)\|_{0,f}^2 \leq \gamma h_P \|v_h\|_P^2 \tag{4.9}$$

where  $\gamma$  is a constant independent of  $v_h, P$  and  $\mathcal{T}_h$  and depending only on  $N_s, \rho_s$ .

**Remark 4.1.** Actually, the properties of the decomposition that we really need are **(C1)–(C4)** and (4.6)–(4.8), and we could take them as our *assumptions* on the decomposition. Readers with a sufficiently solid background in Partial Differential Equations and Functional Analysis will soon recognize that these assumptions require very little regularity properties for the polyhedra in  $\mathcal{T}_h$ . However, in practice, all this generality is not needed, since the decomposition  $\mathcal{T}_h$  is essentially at the choice of the user.

### 5. THE DISCRETE PROBLEM

As it is reasonable to expect, the discrete version of the problem (2.2) will have the following structure

$$\begin{cases} \text{Find } u_h \in \mathcal{N}_0 \text{ such that} \\ [\mathcal{GRAD} u_h, \mathcal{GRAD} v_h]_{\mathcal{E}} = (g, v_h)_{\mathcal{N}} \quad \forall v_h \in \mathcal{N}_0, \end{cases} \tag{5.1}$$

where  $[\cdot, \cdot]_{\mathcal{E}}$  is a suitable scalar product in  $\mathcal{E}_0$  and  $(g, \cdot)_{\mathcal{N}}$  a suitable linear functional on  $\mathcal{N}_0$ , that need to be properly defined.

We shall use the  $H_0^1$ -type inner product  $[u_h, v_h]$  in  $\mathcal{N}_0$  defined by analogy with (2.3),

$$[u_h, v_h] := [\mathcal{GRAD} u_h, \mathcal{GRAD} v_h]_{\mathcal{E}}, \tag{5.2}$$

and write the discrete problem as follows:

$$\begin{cases} \text{Find } u_h \in \mathcal{N}_0 \text{ such that} \\ [u_h, v_h] = (g, v_h)_{\mathcal{N}} \quad \forall v_h \in \mathcal{N}_0. \end{cases} \tag{5.3}$$

#### 5.1. Numerical integration formulae

In order to define the terms appearing in the previous subsection we need to introduce suitable numerical integration formulae. Towards this aim, we choose a numerical integration formula for each element  $P$  and for each face  $f$ . More precisely, for each polyhedron  $P$  with  $V_P$  nodes, we assume that we are given  $V_P$  non-negative weights

$$\omega_P^1, \dots, \omega_P^{V_P} \tag{5.4}$$

such that the corresponding numerical integration formula over  $P$ ,

$$\int_P \chi \, dP \simeq \sum_{i=1}^{V_P} \chi(V_P^i) \omega_P^i, \tag{5.5}$$

is exact whenever  $\chi$  is a constant. Similarly, for every face  $f$  with  $V_f$  nodes, we assume that we are given  $V_f$  non-negative weights

$$\omega_f^1, \dots, \omega_f^{V_f} \tag{5.6}$$

such that the corresponding numerical integration formula over  $f$ ,

$$\int_f \chi \, dS \simeq \sum_{i=1}^{V_f} \chi(V_f^i) \omega_f^i, \tag{5.7}$$

is exact whenever  $\chi$  is a polynomial of degree  $\leq 1$ .

**Remark 5.1.** To derive an integration formula for a face  $f$  which is exact for linear functions, we could use a linear relation expressing the center of mass of  $f$  in terms of its vertices. Since the integral of a linear function equals to the function value at the center of mass times  $|f|$ , the coefficients in the linear expression scaled by  $|f|$  define the weights  $\omega_f^i$ . A similar argument would work for a polyhedron (although it will not be needed here).

5.2. Scalar products

Once we choose our two numerical integration formulae, we can choose the linear functional

$$(g, v_h)_{\mathcal{N}} := \sum_P \bar{g}|_P \sum_{i=1}^{V_P} v_h(V_P^i) \omega_P^i, \tag{5.8}$$

where, in each element  $P$ , we take  $\bar{g}|_P$  as the average of  $g$  over  $P$ , that is

$$\bar{g}|_P := \frac{1}{|P|} \int_P g \, dP. \tag{5.9}$$

In the definition of the scalar product  $[\cdot, \cdot]_{\mathcal{E}}$ , the tensor  $\mathbb{K}$  enters into play and we need to construct a suitable approximation of it. We denote by  $\tilde{\mathbb{K}}$  the piecewise constant tensor on  $\mathcal{T}_h$  obtained by averaging each component of  $\mathbb{K}$  over each element  $P$  in  $\mathcal{T}_h$ . Thus,  $\tilde{\mathbb{K}}$  the  $L^2$ -projection of  $\mathbb{K}$  onto the space of piecewise constant tensors. It is easy to see that

$$\|\mathbb{K} - \tilde{\mathbb{K}}\|_{\infty, P} \leq \gamma h_P, \tag{5.10}$$

where (as we shall assume from now on)  $\gamma$  is a generic constant depending only on  $\mathbb{K}$ , on  $N_s$  and on  $\rho_s$ . For each face  $f$  of  $P$ , we define the outward unit normal vector  $\mathbf{n}_f^P$  and the co-normal vectors

$$\boldsymbol{\nu}_f^P := \mathbb{K}|_P \mathbf{n}_f^P \quad \text{and} \quad \tilde{\boldsymbol{\nu}}_f^P := \tilde{\mathbb{K}}|_P \mathbf{n}_f^P. \tag{5.11}$$

When no confusion will occur, we will simply use  $\boldsymbol{\nu}_f$  and  $\tilde{\boldsymbol{\nu}}_f$  instead of  $\boldsymbol{\nu}_f^P$  and  $\tilde{\boldsymbol{\nu}}_f^P$ , respectively. Using (5.10) it is immediate to see that on each face  $f$

$$\|\boldsymbol{\nu}_f^P - \tilde{\boldsymbol{\nu}}_f^P\|_{\infty, f} \leq \gamma h_P. \tag{5.12}$$

Now, for every polyhedron  $P$ , for every function  $\chi \in H^1(P)$ , and for every polynomial  $p$  of degree  $\leq 1$ , the Gauss-Green formula is

$$\int_P \tilde{\mathbb{K}} \nabla \chi \cdot \nabla p \, dP = \int_{\partial P} \chi \tilde{\mathbb{K}} \nabla p \cdot \mathbf{n} \, dS = \sum_{f \in \partial P} \int_f \chi \frac{\partial p}{\partial \tilde{\boldsymbol{\nu}}_f} \, dS. \tag{5.13}$$

Inspired by (5.13) we make our final choice. For every polyhedron  $P$  we choose a **symmetric** bilinear form  $[u, v]_P$  on  $\mathcal{N}_P \times \mathcal{N}_P$  verifying the following properties:

- For every polynomial  $p$  of degree  $\leq 1$ , setting  $p^I := \Pi_{\mathcal{N}} p$  (as defined in (4.5)), we have

$$[v, p^I]_P \equiv \sum_{f \in \partial P} \sum_{i=1}^{V_f} v(V_f^i) \frac{\partial p}{\partial \tilde{\boldsymbol{\nu}}_f} \omega_f^i \quad \forall v \in \mathcal{N}_P. \tag{5.14}$$

- There exist two constants  $c$  and  $C$  independent of  $P$  and of  $h$  such that

$$c \|v\|_P^2 \leq [v, v]_P \leq C \|v\|_P^2 \quad \forall v \in \mathcal{N}_P. \tag{5.15}$$

Then we set, in a natural way,

$$[\mathcal{G}\mathcal{R}\mathcal{A}\mathcal{D} u, \mathcal{G}\mathcal{R}\mathcal{A}\mathcal{D} v]_{\mathcal{E}} \equiv [u, v] := \sum_P [u, v]_P. \tag{5.16}$$

In Section 7, we show that there exist a family of bilinear forms with the above properties. For the moment, only (5.15) and (5.16) are needed for the convergence analysis.

**Remark 5.2.** Let  $p$  and  $q$  be polynomials of order  $\leq 1$ . Taking into account (5.13) and the fact that the integration formula (5.7) is exact for polynomials of degree  $\leq 1$ , we have immediately that (5.14) implies

$$[\Pi_{\mathcal{N}P} p, \Pi_{\mathcal{N}Q} q]_P = \int_P \tilde{\mathbb{K}} \nabla p \cdot \nabla q \, dP \equiv \int_P \mathbb{K} \nabla p \cdot \nabla q \, dP, \tag{5.17}$$

so that the assumption of symmetry and (5.14) are compatible.

### 5.3. Mimetic finite differences

It is easy to put all this in the framework of Mimetic Finite Differences. The gradient operator  $\mathcal{G}\mathcal{R}\mathcal{A}\mathcal{D}$  is the *primary* operator, and the divergence operator  $\mathcal{D}\mathcal{J}\mathcal{V}_{\mathbb{K}}$  is the *derived* operator. Operators  $\mathcal{G}\mathcal{R}\mathcal{A}\mathcal{D}$  and  $\mathcal{D}\mathcal{J}\mathcal{V}_{\mathbb{K}}$  approximate operators  $\mathbf{grad} \cdot$  and  $\text{div}(\mathbb{K} \cdot)$ , respectively. Let  $[\cdot, \cdot]_{\mathcal{N}}$  be a suitable scalar product in  $\mathcal{N}$ . The divergence operator is formally defined through the discrete Green formula:

$$[\mathcal{D}\mathcal{J}\mathcal{V}_{\mathbb{K}} G_h, v_h]_{\mathcal{N}} = -[G_h, \mathcal{G}\mathcal{R}\mathcal{A}\mathcal{D} v_h]_{\mathcal{E}} \quad \forall G_h \in \mathcal{E}_0, v_h \in \mathcal{N}_0. \tag{5.18}$$

Then, the MFD method is

$$\begin{cases} \text{Find } u_h \in \mathcal{N}_0 \text{ and } G_h \in \mathcal{E}_0 \text{ such that} \\ G_h = \mathcal{G}\mathcal{R}\mathcal{A}\mathcal{D} u_h, \\ \mathcal{D}\mathcal{J}\mathcal{V}_{\mathbb{K}} G_h = -\Pi_{\mathcal{N}_0}(g). \end{cases} \tag{5.19}$$

For a more general framework on Cochain approximations of Differential Forms (that however does not include the present discussion), see [3].

## 6. ERROR ESTIMATES

We point out that our choices of the scalar product  $[\cdot, \cdot]$  and of the linear functional  $(g, \cdot)_{\mathcal{N}}$  depend on three choices:

- the integration formula (5.5) in each polyhedron  $P$ ;
- the integration formula (5.7) on each face  $f$ ;
- the bilinear forms  $[u, v]_P$  for each  $P$ .

All the properties of the numerical scheme, including *a priori* error estimates, will be derived by the properties of the integration formulae and of the bilinear forms defining the scalar product.

Let  $u_h$  be the solution of the discrete problem (5.3) and  $u$  be the solution of the continuous problem (2.2). We assume that  $u \in \mathcal{H}^1(\Omega)$  and set  $u^I = \Pi_{\mathcal{N}} u$ . We shall also consider the discontinuous function  $w$  which is linear in each polyhedron  $P$  of  $\mathcal{T}_h$ . The restriction of  $w$  to  $P$ , denoted by  $w_P$ , is defined as the  $L^2(P)$ -projection of  $u$  onto the space of polynomials of degree  $\leq 1$ . We shall also denote by  $w_P^I$  the element of  $\mathcal{N}_P$  that assumes the values of  $w_P$  at the nodes of  $P$ .

Finally, we set

$$\delta := u_h - u^I \tag{6.1}$$

and estimate  $\delta$  in the norm  $\|\cdot\|$ .



6.1. Six easy pieces

We have

$$\begin{aligned}
 c \|\delta\|^2 &= c \sum_P \|\delta\|_P^2 && \text{(use (5.15) and (5.16))} \\
 &\leq [\delta, \delta] && \text{(use (6.1))} \\
 &= [u_h, \delta] - [u^I, \delta] && \text{(use (5.3))} \\
 &= (g, \delta)_N - [u^I, \delta] \equiv II - [u^I, \delta].
 \end{aligned} \tag{6.2}$$

On the other hand, starting with (5.16), we get

$$\begin{aligned}
 [u^I, \delta] &= \sum_P [u^I, \delta]_P && \text{(add and subtract } w_P^I) \\
 &= \sum_P [u^I - w_P^I, \delta]_P + \sum_P [w_P^I, \delta]_P \\
 &\equiv II + \sum_P [w_P^I, \delta]_P && \text{(use (5.14))} \\
 &= II + \sum_P \sum_{f \in \partial P} \sum_{i=1}^{V_f} \delta(V_f^i) \frac{\partial w_P}{\partial \tilde{\nu}_f} \omega_i^f.
 \end{aligned} \tag{6.3}$$

Moreover, for every  $P \in \mathcal{T}_h$  and for every face  $f \in \partial P$ , using that (5.7) is exact on constants, we have

$$\begin{aligned}
 \sum_{i=1}^{V_f} \delta(V_f^i) \frac{\partial w_P}{\partial \tilde{\nu}_f} \omega_i^f &= \sum_{i=2}^{V_f} [\delta(V_f^i) - \delta(V_f^1)] \frac{\partial w_P}{\partial \tilde{\nu}_f} \omega_i^f + \sum_{i=1}^{V_f} \delta(V_f^1) \frac{\partial w_P}{\partial \tilde{\nu}_f} \omega_i^f \\
 &= \sum_{i=2}^{V_f} [\delta(V_f^i) - \delta(V_f^1)] \frac{\partial w_P}{\partial \tilde{\nu}_f} \omega_i^f + \int_f \delta(V_f^1) \frac{\partial w_P}{\partial \tilde{\nu}_f} dS.
 \end{aligned}$$

Thus,

$$\begin{aligned}
 \sum_P \sum_{f \in \partial P} \sum_{i=1}^{V_f} \delta(V_f^i) \frac{\partial w_P}{\partial \tilde{\nu}_f} \omega_i^f &= \sum_P \sum_{f \in \partial P} \sum_{i=2}^{V_f} [\delta(V_f^i) - \delta(V_f^1)] \frac{\partial w_P}{\partial \tilde{\nu}_f} \omega_i^f + \sum_P \sum_{f \in \partial P} \int_f \delta(V_f^1) \frac{\partial w_P}{\partial \tilde{\nu}_f} dS \\
 &\equiv III + \sum_P \sum_{f \in \partial P} \int_f \delta(V_f^1) \frac{\partial w_P}{\partial \tilde{\nu}_f} dS.
 \end{aligned}$$

We can now add and subtract a function  $R_N(\delta) \in \mathcal{H}^1(\Omega)$  that, for the moment, is just *any function* in  $\mathcal{H}^1(\Omega)$  having the same value as  $\delta$  at the nodes. Later, we shall require that it satisfies (4.6)–(4.8). We obtain

$$\begin{aligned}
 \sum_P \sum_{f \in \partial P} \int_f \delta(V_f^1) \frac{\partial w_P}{\partial \tilde{\nu}_f} dS &&& \text{(add and subtract } R_N(\delta)) \\
 &= \sum_P \sum_{f \in \partial P} \int_f [\delta(V_f^1) - R_N(\delta)] \frac{\partial w_P}{\partial \tilde{\nu}_f} dS + \sum_P \sum_{f \in \partial P} \int_f R_N(\delta) \frac{\partial w_P}{\partial \tilde{\nu}_f} dS \\
 &\equiv IV + \sum_P \sum_{f \in \partial P} \int_f R_N(\delta) \frac{\partial w_P}{\partial \tilde{\nu}_f} dS && \text{(use (5.13))} \\
 &= IV + \sum_P \int_P \tilde{\mathbb{K}} \nabla R_N(\delta) \cdot \nabla w_P dP.
 \end{aligned} \tag{6.4}$$

Finally,

$$\begin{aligned}
 & \sum_P \int_P \tilde{\mathbb{K}} \nabla R_{\mathcal{N}}(\delta) \cdot \nabla w_P dP && \text{(add and subtract } \nabla u) \\
 &= \sum_P \int_P \tilde{\mathbb{K}} \nabla R_{\mathcal{N}}(\delta) \cdot \nabla (w_P - u) dP + \int_{\Omega} \tilde{\mathbb{K}} \nabla R_{\mathcal{N}}(\delta) \cdot \nabla u dP \\
 &\equiv V + \int_{\Omega} \tilde{\mathbb{K}} \nabla R_{\mathcal{N}}(\delta) \cdot \nabla u dP && \text{(add and subtract } \mathbb{K}) \tag{6.5} \\
 &= V + \int_{\Omega} (\tilde{\mathbb{K}} - \mathbb{K}) \nabla R_{\mathcal{N}}(\delta) \cdot \nabla u dP + \int_{\Omega} \mathbb{K} \nabla R_{\mathcal{N}}(\delta) \cdot \nabla u dP && \text{(use (2.2))} \\
 &\equiv V + VI + \int_{\Omega} gR_{\mathcal{N}}(\delta) dP.
 \end{aligned}$$

Collecting the above equations, we have

$$\begin{aligned}
 c \|\delta\|^2 \leq & \left\{ (g, \delta)_{\mathcal{N}} - \int_{\Omega} gR_{\mathcal{N}}(\delta) dP \right\} - \sum_P [u^I - w_P^I, \delta]_P \\
 & - \sum_P \sum_{f \in \partial P} \sum_{i=2}^{V_f} [\delta(V_f^i) - \delta(V_f^1)] \frac{\partial w_P}{\partial \tilde{\nu}_f} \omega_f^i - \sum_P \sum_{f \in \partial P} \int_f [\delta(V_f^1) - R_{\mathcal{N}}(\delta)] \frac{\partial w_P}{\partial \tilde{\nu}_f} dS \\
 & - \sum_P \int_P \tilde{\mathbb{K}} \nabla R_{\mathcal{N}}(\delta) \cdot \nabla (w_P - u) dP - \int_{\Omega} (\tilde{\mathbb{K}} - \mathbb{K}) \nabla R_{\mathcal{N}}(\delta) \cdot \nabla u dP. \tag{6.6}
 \end{aligned}$$

In the next section, we shall estimate separately each of the Six Easy Pieces in the above equation.

### 6.2. Four useful lemmata

We shall need four simple lemmata. Let  $\omega_P^i$  and  $\omega_f^i$  be such that (5.5) and (5.7) are exact for constant and linear functions, respectively.

**Lemma 6.1.** *There exist a constant  $\gamma_1$ , depending only on  $N_s$  and  $\rho_s$ , such that, for every polyhedron  $P$ , for every vertex  $V_P^i$  of  $P$ , and for every  $\chi$  in  $\mathcal{N}_P$ :*

$$\sum_{V_P^i \in P} [\chi(V_P^1) - \chi(V_P^i)]^2 \omega_P^i \leq \gamma_1 h_P^2 \|\chi\|_P^2. \tag{6.7}$$

*Proof.* Since all the  $\omega_P^i$  are non-negative and their sum is  $|P|$ , then every  $\omega_P^i$  is bounded by  $h_P^3$ . Then the triangle inequality, and the fact that in every  $P$  we have less than  $N_v$  vertices (from **(C1)**), easily imply the result. □

**Lemma 6.2.** *There exists a constant  $\gamma_2$ , depending only on  $N_s$  and  $\rho_s$ , such that for every polyhedron  $P$ , for every face  $f$  of  $P$ , for every vertex  $V_f^1$  of  $f$ , and for every  $\chi$  in  $\mathcal{N}_P$ :*

$$\sum_{V_f^i \in f} [\chi(V_f^1) - \chi(V_f^i)]^2 \omega_f^i \leq \gamma_2 h_P \|\chi\|_P^2. \tag{6.8}$$

*Proof.* The proof is the same as before; but this time every  $\omega_f^i$  is bounded by  $h_P^2$ . □

**Lemma 6.3.** *Let  $\varphi \in H^2(\Omega) \cap H_0^1(\Omega)$ , and let  $\varphi^I$  be the continuous piecewise linear interpolant of  $\varphi$  on the grid  $\mathcal{S}_h$ . Let  $\psi$ , piecewise linear (and discontinuous) on the partition  $\mathcal{T}_h$ , be defined as follows: for every  $P \in \mathcal{T}_h$ ,  $\psi_P$  is the  $L^2(P)$ -projection of  $\varphi$  over the polynomials of degree  $\leq 1$ . For every  $P \in \mathcal{T}_h$  we denote as well (with an abuse of notation) by  $\varphi^I$  and  $\psi_P$  the elements in  $\mathcal{N}_P$  that assume the same values of  $\varphi$  and  $\psi_P$  (respectively) at the vertices of  $P$ . Then*

$$\|\varphi^I - \psi_P\|_P^2 \leq \gamma_3 h_P^2 |\varphi|_{2,P}^2 \tag{6.9}$$

where  $\gamma_3$  depends only on  $N_s$  and  $\rho_s$ .

*Proof.* As both  $\varphi^I$  and  $\psi_P$  are piecewise linear on the regular grid  $\mathcal{S}_{h|P}$ , we can use all the classical finite element tools (including inverse inequalities). In particular,

$$\left[|\varphi^I - \psi_P, \varphi^I - \psi_P|\right]_P^{1/2} = \|\varphi^I - \psi_P\|_P \leq \gamma |\varphi^I - \psi_P|_{1,P}. \tag{6.10}$$

Moreover,

$$|\varphi^I - \psi_P|_{1,P} \leq \gamma h_P^{-1} \|\varphi^I - \psi_P\|_{0,P} \leq \gamma h_P^{-1} (\|\varphi^I - \varphi\|_{0,P} + \|\varphi - \psi_P\|_{0,P}) \leq \gamma h_P |\varphi|_{2,P}.$$

The last step above requires additional comments. At a first sight, the estimate of the term  $\|\varphi - \psi_P\|_{0,P}$  may depend upon the shape of  $P$  which is a generic polyhedron. However one can argue as follows. Polyhedron  $P$  is the star-shaped domain with respect to a ball of radius  $\rho_s^* h_P$  where the constant  $\rho_s^*$  depends on various constants appeared in **(C1)**–**(C3)**. Is also satisfies the strong cone condition. Then the result follows from the revised Bramble-Hilbert lemma for star-shaped domains [2].  $\square$

**Lemma 6.4.** *In the same assumptions of the previous lemma, for each internal face  $f$  (common to the two polyhedra  $P_1$  and  $P_2$ ), we define*

$$j_f(\psi) := |\nabla \psi_{P_1} \cdot \tilde{\nu}_f^{P_1} + \nabla \psi_{P_2} \cdot \tilde{\nu}_f^{P_2}|. \tag{6.11}$$

Then,

$$\sum_{f \in \mathcal{F}_0(\mathcal{T}_h)} \|j_f(\psi)\|_{0,f}^2 \leq \gamma_4 \sum_{P \in \mathcal{T}_h} h_P |\varphi|_{2,P}^2, \tag{6.12}$$

where  $\gamma_4$  depends only on  $N_s$ ,  $\rho_s$ , and  $\mathbb{K}$ .

*Proof.* By our assumptions,  $\mathbb{K} \nabla \varphi$  is continuous, so that, recalling the definition (5.11), on each internal face it holds:

$$\nabla \varphi \cdot \nu_f^{P_1} + \nabla \varphi \cdot \nu_f^{P_2} = 0. \tag{6.13}$$

Using (5.12) and the Agmon inequality (3.5), we have

$$\|\nabla \varphi \cdot \tilde{\nu}_f^{P_1} + \nabla \varphi \cdot \tilde{\nu}_f^{P_2}\|_{0,f}^2 \leq \gamma (h_{P_1} \|\varphi\|_{2,P_1}^2 + h_{P_2} \|\varphi\|_{2,P_2}^2). \tag{6.14}$$

We have, with obvious notation

$$j_f(\psi) \leq |\nabla(\psi_{P_1} - \varphi) \cdot \tilde{\nu}_f^{P_1}| + |\nabla(\psi_{P_2} - \varphi) \cdot \tilde{\nu}_f^{P_2}| + |\nabla \varphi \cdot \tilde{\nu}_f^{P_1} + \nabla \varphi \cdot \tilde{\nu}_f^{P_2}|. \tag{6.15}$$

Using again the Agmon inequality (3.5) we have (for  $i = 1, 2$ ):

$$\|\nabla(\psi_{P_i} - \varphi) \cdot \tilde{\nu}_f\|_{0,f}^2 \leq \gamma \|\tilde{\nu}_f\|^2 \left( h_{P_i}^{-1} |\psi_{P_i} - \varphi|_{1,P_i}^2 + h_{P_i} |\varphi|_{2,P_i}^2 \right) \leq \gamma h_{P_i} |\varphi|_{2,P_i}^2, \tag{6.16}$$

and (6.12) follows.  $\square$

### 6.3. Estimate of each piece

We begin by observing that for each  $P$  and for each vertex  $W_P$  of  $P$ , we easily have

$$\bar{g}_P \sum_i \omega_P^i \delta(W_P) = \bar{g}_P \int_P \delta(W_P) dP = \int_P g \delta(W_P) dP. \tag{6.17}$$

Hence, the *First Piece* is bounded by

$$\begin{aligned} & |(g, \delta)_{\mathcal{N}} - \int_{\Omega} g R_{\mathcal{N}}(\delta) dP| \tag{use (5.8)} \\ &= \sum_P \bar{g}_P \sum_i \omega_P^i \delta(V_P^i) - \int_{\Omega} g R_{\mathcal{N}}(\delta) dP \tag{add and subtract} \int_P g \delta(V_P^1) dP \\ &= \sum_P \bar{g}_P \sum_i \omega_P^i (\delta(V_P^i) - \delta(V_P^1)) - \sum_P \int_P g (R_{\mathcal{N}}(\delta) - \delta(V_P^1)) dP \tag{use (6.7)} \\ &\leq \gamma \|g\|_{0,\Omega} \sum_P (h_P^2 \|\delta\|_P^2)^{1/2} - \sum_P \int_P g (R_{\mathcal{N}}(\delta) - \delta(V_P^1)) dP \tag{use (4.8)} \\ &\leq \gamma \|g\|_{0,\Omega} \sum_P (h_P^2 \|\delta\|_P^2)^{1/2} \leq \gamma \|g\|_{0,\Omega} |h| \|\delta\|. \end{aligned}$$

Using (6.9), we see that the *Second Piece* is bounded by

$$\left| \sum_P [u^I - w_P^I, \delta]_P \right| \leq \sum_P \|u^I - w_P^I\|_P \|\delta\|_P \leq \gamma \left( \sum_P h_P^2 |u|_{2,P}^2 \right)^{1/2} \|\delta\| \leq \gamma |h| |u|_{2,\Omega} \|\delta\|.$$

In order to estimate the third piece, we remark first that  $\delta$  is equal to zero on each vertex belonging to  $\partial\Omega$ . Hence, we can consider only the *internal faces*. Taking also into account that  $\delta$  is single valued, we first rearrange terms to get

$$\left| \sum_P \sum_{f \in \partial P} \sum_{i=2}^{V_f} [\delta(V_f^i) - \delta(V_f^1)] \frac{\partial w_P}{\partial \bar{\nu}_f} \omega_i^f \right| \leq \sum_{f \in \mathcal{F}_0(\mathcal{T}_h)} \sum_{i=2}^{V_f} |\delta(V_f^i) - \delta(V_f^1)| |j_f(w) \omega_i^f|. \tag{6.18}$$

Then, we use Cauchy-Schwartz, estimate (6.8), the fact that the integration formula is exact on constants, and finally (6.12) to get

$$\begin{aligned} & \sum_{f \in \mathcal{F}_0(\mathcal{T}_h)} \sum_{i=2}^{V_f} |\delta(V_f^i) - \delta(V_f^1)| |j_f(w) \omega_i^f| \\ & \leq \left( \sum_P \sum_{f \in \partial P} \sum_{i=2}^{V_f} [\delta(V_f^i) - \delta(V_f^1)]^2 \omega_i^f \right)^{1/2} \left( \sum_{f \in \mathcal{F}_0(\mathcal{T}_h)} \sum_{i=1}^{V_f} |j_f(w)|^2 \omega_i^f \right)^{1/2} \\ & \leq \gamma \left( \sum_P h_P \|\delta\|_P^2 \right)^{1/2} \left( \sum_{f \in \mathcal{F}_0(\mathcal{T}_h)} \|j_f(w)\|_{0,f}^2 \right)^{1/2} \\ & \leq \gamma \left( \sum_P h_P \|\delta\|_P^2 \right)^{1/2} \left( \sum_P h_P |u|_{2,P}^2 \right)^{1/2} \leq \gamma |h| \|\delta\| |u|_{2,\Omega} \end{aligned}$$

that joined with (6.18) gives the estimate of the *Third Piece*:

$$\left| \sum_P \sum_{f \in \partial P} \sum_{i=2}^{V_f} [\delta(V_f^i) - \delta(V_f^1)] \frac{\partial w_P}{\partial \tilde{\mathbf{v}}_f} \omega_i^f \right| \leq \gamma |h| \|\delta\| |u|_{2,\Omega}. \tag{6.19}$$

Following essentially the estimate of the third piece and just using (4.9) instead of (6.8), we can estimate the *Fourth Piece*:

$$\begin{aligned} \sum_P \sum_{f \in \partial P} \int_f [\delta(V_f^1) - R_{\mathcal{N}}(\delta)] \frac{\partial w_P}{\partial \tilde{\mathbf{v}}_f} dP &\leq \sum_{f \in \mathcal{F}_0(\mathcal{T}_h)} \int_f |\delta(V_f^1) - R_{\mathcal{N}}(\delta)| |j_f(w)| dP \\ &\leq \gamma \left( \sum_P h_P \|\delta\|_P^2 \right)^{1/2} \left( \sum_P h_P |u|_{2,P}^2 \right)^{1/2} \\ &\leq \gamma |h| \|\delta\| |u|_{2,\Omega}. \end{aligned} \tag{6.20}$$

We can estimate the *Fifth Piece* using (4.7) and the usual approximation results:

$$\left| \sum_P \int_P \tilde{\mathbb{K}} \nabla R_{\mathcal{N}}(\delta) \cdot \nabla (w_P - u) dP \right| \leq \gamma |R_{\mathcal{N}}(\delta)|_{1,\Omega} \left( \sum_P h_P^2 |u|_{2,P}^2 \right)^{1/2} \leq \gamma |h| \|\delta\| |u|_{2,\Omega}.$$

Finally, for the *Sixth Piece*, we use (5.10) and (4.7) to obtain:

$$\int_{\Omega} (\tilde{\mathbb{K}} - \mathbb{K}) \nabla R_{\mathcal{N}}(\delta) \cdot \nabla u dP \leq \gamma |h| \|\delta\| |u|_{1,\Omega}.$$

Thus, we proved the following theorem.

**Theorem 6.5.** *Let  $\Omega$  be a bounded Lipschitz polyhedron and  $\mathbb{K}$  be a  $W^{1,\infty}(\Omega)$  symmetric tensor. Furthermore, let the sequence of decompositions  $\mathcal{T}_h$  satisfy assumption **(HG)**, and the discrete inner product (5.16) satisfy (5.14) and (5.15). Finally, let  $u$  and  $u_h$  be solutions of (2.2) and (5.3), respectively, and  $u^I = \Pi_{\mathcal{N}} u$ . Then,*

$$\|u^I - u_h\| \leq \gamma |h| (\|g\|_{0,\Omega} + |u|_{1,\Omega} + |u|_{2,\Omega}),$$

where  $\gamma$  depends only on  $N_s$ ,  $\rho_s$  and  $\mathbb{K}$ .

## 7. NUMERICAL RESULTS

### 7.1. Algebraic issues

In this section, we construct explicitly the bilinear form  $[v, u]_P$  on  $\mathcal{N}_P \times \mathcal{N}_P$  verifying (5.14) and (5.15).

Let the polyhedron  $P$  have  $n_v$  vertices. Our definition of the bilinear form implies that we have to construct a symmetric positive definite  $n_v \times n_v$  matrix  $\mathbb{M}_P$  such that

$$[v, u]_P = \mathbf{v}^T \mathbb{M}_P \mathbf{u},$$

where  $\mathbf{v}$  and  $\mathbf{u}$  are vectors in  $\mathbb{R}^{n_v}$  with entries  $u(V)$  and  $v(V)$ , respectively,  $V \in P$ . In each  $\mathcal{N}_P$  we construct a new basis as follows. The first four elements of the new basis will be the nodal values of the polynomials of degree  $\leq 1$ :

$$B_1 = \Pi_{\mathcal{N}} 1, \quad B_{i+1} = \Pi_{\mathcal{N}}(x_i - x_i^P) \quad i = 1, 2, 3, \tag{7.1}$$

where  $\mathbf{x}^P$  is the barycenter of  $P$ . Using (5.17), we have immediately

$$[B_1, v]_P = 0 \quad \forall v \in \mathcal{N}_P \tag{7.2}$$

and

$$[B_{i+1}, B_{j+1}]_P = \tilde{\mathbb{K}}_{i,j}|P| \quad i, j = 1, 2, 3. \tag{7.3}$$

Moreover, using (5.14), we have that the scalar product  $[v, B_i]_P$  can be computed in a unique way, for every  $v \in \mathcal{N}_P$  and  $i = 1, \dots, 4$ . Hence, the problem of finding linearly independent  $B_k, k = 5, \dots, n_v$ , such that

$$[B_i, B_k]_P = 0 \tag{7.4}$$

for  $i = 1, \dots, 4$  and  $k = 5, \dots, n_v$  makes perfect sense. To simplify the following discussion, we can also assume that the  $B_k$  are normalized by

$$\|B_k\|_P^2 = |P| \quad k = 5, \dots, n_v.$$

Let  $\mathbf{B}_i, i = 1, \dots, n_v$ , be vectors in  $\mathfrak{R}^{n_v}$  with entries  $B_k(V)$ , for any vertex  $V$  of  $P$ . If  $\tilde{\mathbb{M}}_P$  is the matrix that represents our scalar product in the new basis  $\mathbf{B}_1, \dots, \mathbf{B}_{n_v}$ , from (5.17) and (7.4) we already know explicitly the first four lines and the first four columns of  $\tilde{\mathbb{M}}_P$ . Hence, we only have to decide the  $(n_v - 4) \times (n_v - 4)$  block at the bottom-right. It is easy to see that every symmetric and positive definite matrix  $\mathbb{U}$  that satisfies (5.15) will do. For instance we can take

$$\mathbb{U} = \text{trace}(\tilde{\mathbb{K}}) |P| \mathbb{I}_{n_v-4}$$

where  $\mathbb{I}_{n_v-4}$  is the identity matrix in  $n_v - 4$  dimensions. Hence,  $\tilde{\mathbb{M}}_P$  will be given by

$$\tilde{\mathbb{M}}_P = \begin{bmatrix} 0 & 0 & 0 \\ 0 & \tilde{\mathbb{K}}|P| & 0 \\ 0 & 0 & \mathbb{U} \end{bmatrix}. \tag{7.5}$$

Returning to the original basis, we get

$$\mathbb{M}_P = \mathbb{B}^{-T} \tilde{\mathbb{M}}_P \mathbb{B}^{-1}, \quad \mathbb{B} = [\mathbf{B}_1, \dots, \mathbf{B}_{n_v}]. \tag{7.6}$$

**Remark 7.1.** In the case of tetrahedral meshes, the matrix  $\mathbb{M}_P$  coincides with the stiffness matrix in the standard  $P_1$  finite element method.

In practice, we avoid inversion of matrix  $\mathbb{B}$  using different representation of a family of admissible matrices  $\mathbb{M}_P$ . Following essentially [5], we define vectors  $\mathbf{A}_i, i = 2, 3, 4$ , as follows:

$$\mathbf{A}_i = \mathbb{M}_P \mathbf{B}_i.$$

The vectors  $\mathbf{A}_i$  can be calculated directly from the right-hand side of (5.14). Formula (7.3) implies that

$$\mathbf{A}_{i+1}^T \mathbf{B}_{j+1} = \tilde{\mathbb{K}}_{i,j}|P|, \quad i, j = 1, 2, 3.$$

Let  $\mathbb{A}_1$  be a  $n_v \times 3$  matrix with columns  $\mathbf{A}_i, i = 2, 3, 4$ , and  $\mathbb{B}_1$  be a  $n_v \times 4$  matrix with columns  $\mathbf{B}_i, i = 1, \dots, 4$ . Furthermore, let  $\mathbb{D}_1$  be a  $n_v \times (n_v - 4)$  matrix with columns that span the null space of  $\mathbb{B}_1^T$ , i.e.  $\mathbb{B}_1^T \mathbb{D}_1 = 0$ . Then, the general form of the matrix  $\mathbb{M}_P$  is (see [5] for more details)

$$\mathbb{M}_P = \frac{1}{|P|} \mathbb{A}_1 \tilde{\mathbb{K}}^{-1} \mathbb{A}_1^T + \mathbb{D}_1 \tilde{\mathbb{U}} \mathbb{D}_1^T, \tag{7.7}$$

where  $\tilde{\mathbb{U}}$  is an arbitrary  $(n_v - 4) \times (n_v - 4)$  symmetric positive definite matrix.

TABLE 1. Convergence rates on hexahedral meshes.

FEM method		MFD method	
$n_P$	$\epsilon(u^I, u_h)$	$n_P$	$\epsilon(u^I, u_h)$
1536	1.98 e-1	1536	3.49 e-1
12 288	1.23 e-1	12 288	1.99 e-1
98 304	6.99 e-2	98 304	1.01 e-1
786 432	3.58 e-2	786 432	5.11 e-2
rate:	0.83	rate:	0.98

In numerical experiments, we use a scalar matrix  $\tilde{\mathbb{U}}$  and replace matrix  $\mathbb{D}_1$  with the orthogonal projector onto the null space of  $\mathbb{B}_1^T$ :

$$\mathbb{M}_P = \frac{1}{|P|} \mathbb{A}_1 \tilde{\mathbb{K}}^{-1} \mathbb{A}_1^T + \text{trace}(\tilde{\mathbb{K}}) |P| (\mathbb{I}_{n_v} - \mathbb{B}_1 (\mathbb{B}_1^T \mathbb{B}_1)^{-1} \mathbb{B}_1^T). \quad (7.8)$$

Since vector  $\mathbf{B}_1$  is orthogonal to vectors  $\mathbf{B}_i$ ,  $i = 2, 3, 4$ , the matrix  $\mathbb{B}_1^T \mathbb{B}_1$  is block diagonal. Thus, (7.6) require inversion of only a  $3 \times 3$  matrix.

## 7.2. Model problem with a full tensor

We consider the Dirichlet boundary value problem (2.1) with the exact solution

$$u(x, y, z) = x^3 y^2 z + x \sin(2\pi xy) \sin(2\pi yz) \sin(2\pi z)$$

and the full diffusion tensor

$$\mathbb{K} = \begin{pmatrix} y^2 + z^2 + 1 & -xy & -xz \\ -xy & x^2 + z^2 + 1 & -yz \\ -xz & -yz & x^2 + y^2 + 1 \end{pmatrix}.$$

We consider two sequences  $\{\mathcal{J}_h\}_h$  of meshes. The first sequence of non-smooth hexahedral meshes is built in a unit cube using two steps. First, each cell of a cubic mesh is split into six tetrahedra. Second, each tetrahedron is split into four hexahedra using its vertices, centers of edges and faces, and the center of mass. One of the meshes in the sequence is shown on the left picture in Figure 2.

The second sequences of polyhedral meshes with slightly curved faces is built in a spherical layer with the interior radius 1 and the exterior radius 2 (see the right picture in Fig. 2). The mesh consists of prisms with hexagonal and pentagonal bases. In both sequences, the number of elements in  $\mathcal{J}_h$  is increased roughly 8 times which corresponds to a two-fold reduction of  $|h|_{\mathcal{J}_h}$ .

The results of numerical experiments are collected in Tables 1 and 2. The theoretically predicted first-order convergence rate for  $\|u^I - u_h\|$  is observed in both experiments. The linear regression algorithm has been used to calculate the convergence rate. The following relative error is calculated in numerical experiments:

$$\epsilon(u^I, u_h) = \frac{\|u^I - u_h\|}{\|u^I\|}.$$

For a hexahedral mesh, we compare our method with the trilinear finite element (FEM) method. To a fairer comparison, the piecewise constant diffusion tensor  $\tilde{\mathbb{K}}$  has been used in the finite element code. Fifth degree Gauss quadrature has been used for calculating finite element elemental stiffness matrices. Table 1 shows that the MFD method achieves asymptotic convergence faster than the FEM method; however, it produces 1.4 larger

TABLE 2. Convergence rates on polyhedral meshes.

MFD method		FEM method	
$n_P$	$\epsilon(u^I, u_h)$	$n_P$	$\epsilon(u^I, u_h)$
486	1.66	5724	1.38
3852	1.09	46 008	0.45
30 744	0.48	368 496	0.19
245 808	0.23	2 948 832	0.09
rate:	0.98	rate:	1.30

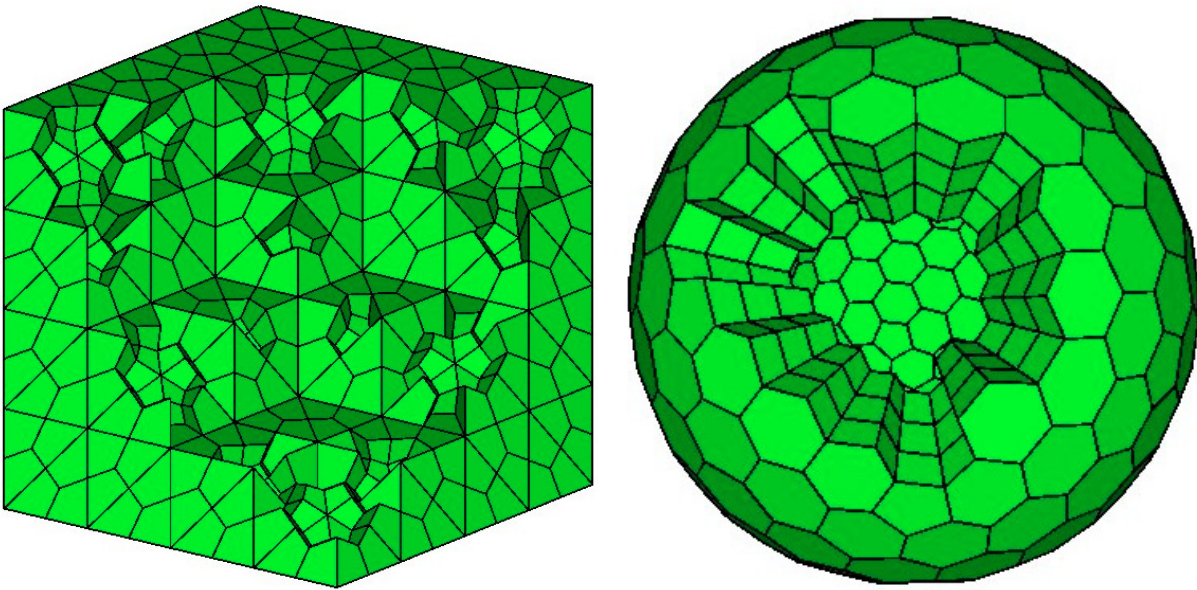


FIGURE 2. Unstructured non-smooth hexahedral mesh (left picture) and polyhedral mesh with slightly curved faces (right picture). Part of the mesh has been removed to show the interior structure.

error on the finest mesh. Since the numerical integration makes the FEM method more expensive, the total cost-accuracy depends on efficiency of the employed iterative solver.

For a polyhedral (prismatic) mesh, we compare our method with the FEM method on a tetrahedral mesh having the same nodes. To build the tetrahedral mesh, we first split each polyhedron into a few triangular prisms and then split each prism into three tetrahedra. An alternative approach would be to generate the constrained Delaunay mesh. However, structure of our prismatic mesh (see Fig. 2) is such that the simpler approach also results in a good quality mesh. Note that the number of elements in a tetrahedral mesh is about 12 times larger than in the corresponding polyhedral mesh. In the FEM method, the diffusion tensor is approximated by a piecewise constant tensor on the tetrahedral mesh. This may explain the faster convergence of this method on coarser meshes. As the result, the linear regression algorithm overestimates the convergence rate (see Tab. 2).

For polyhedral meshes, the arbitrary matrix  $\mathbb{U}$  in (7.5) or the matrix  $\tilde{\mathbb{U}}$  in (7.7) may be a full symmetric matrix with many free parameters (10 for hexahedral meshes). The optimal (in a sense of the method accuracy) choice of these parameters is still an open question.



To preserve an underlying cylindrical or spherical symmetry, special meshes respecting this symmetry are frequently used in simulations. For such meshes, that a special choice of the matrix  $\tilde{U}$  in (7.7) may result in a method which improves (or even preserves) the symmetry. This conjecture will be analyzed in the future.

## APPENDIX A – CONSTRUCTION OF THE LIFTING

We consider now the problem of constructing lifting operators  $v_h \rightarrow R_{\mathcal{N}}v_h$  from  $\mathcal{N}$  into  $\mathcal{H}^1(\Omega)$  with the following properties:

- For every  $v_h \in \mathcal{N}$ ,

$$\Pi_{\mathcal{N}}R_{\mathcal{N}}v_h = v_h. \quad (\text{A.1})$$

- For every  $v_h \in \mathcal{N}_0$  and for every polyhedron  $P \in \mathcal{T}_h$ ,

$$\|R_{\mathcal{N}}v_h\|_{1,P} \leq \gamma h_P \sum_{e \in \partial P} \left| \left( \mathcal{G}\mathcal{R}\mathcal{A}\mathcal{D}_P v_h \right) \Big|_e \right|^2 = \gamma \|v_h\|_P^2 \quad (\text{A.2})$$

where, again,  $\gamma$  denotes a constant that depends solely on  $N_s$  and  $\rho_s$ .

- For every  $v_h \in \mathcal{N}_0$ , for every polyhedron  $P \in \mathcal{T}_h$  and for every vertex  $V \in P$ ,

$$\|R_{\mathcal{N}}v_h - v_h(V)\|_{0,P}^2 \leq \gamma h_P^3 \sum_{e \in \partial P} \left| \left( \mathcal{G}\mathcal{R}\mathcal{A}\mathcal{D}_P v_h \right) \Big|_e \right|^2 = \gamma h_P^2 \|v_h\|_P^2. \quad (\text{A.3})$$

It will be convenient to introduce some additional notation. If  $Q$  is a geometric object, we denote by  $\mathcal{V}(\mathcal{S}_h, Q)$  the set of vertices of  $\mathcal{S}_h$  that belong to  $\bar{Q}$  (the closure of  $Q$ ), and by  $\mathcal{V}_0(\mathcal{S}_h, Q)$  the set of vertices of  $\mathcal{S}_h$  that are *internal* to  $Q$ . Moreover, for each vertex  $V \in \mathcal{V}_0(\mathcal{S}_h, Q)$ , we denote by  $\mathcal{V}_{(\mathcal{S}_h, Q)}(V)$  the set of vertices in  $\mathcal{V}(\mathcal{S}_h, Q)$  sharing an edge with  $V$  and being different from  $V$ .

We begin our construction by defining first  $R_{\mathcal{N}}v_h$  on each edge of  $\mathcal{T}_h$ . For each edge  $e$ , we consider its quasi-uniform decomposition  $\mathcal{S}_h|_e$  into sub-intervals of comparable length (due to assumption **(HG)**). The two endpoints  $V_e^1$  and  $V_e^2$  of  $e$  are always vertices of the (coarser) decomposition  $\mathcal{T}_h$ . We assign the values at these endpoints of  $e$ :

$$R_{\mathcal{N}}v_h(V_e^i) = v_h(V_e^i), \quad i = 1, 2. \quad (\text{A.4})$$

Then, we consider the system

$$\sum_{W \in \mathcal{V}_{(\mathcal{S}_h, e)}(V)} [R_{\mathcal{N}}v_h(V) - R_{\mathcal{N}}v_h(W)] = 0 \quad \forall V \in \mathcal{V}_0(\mathcal{S}_h, e), \quad (\text{A.5})$$

where the unknowns are clearly the values of  $R_{\mathcal{N}}v_h$  in  $\mathcal{V}_0(\mathcal{S}_h, e)$ , while the values at the endpoints are given by (A.4). Note that if  $W_1$  and  $W_2$  are the two elements of  $\mathcal{V}_{(\mathcal{S}_h, e)}(V)$ , then

$$R_{\mathcal{N}}v_h(V) = \frac{1}{2}(R_{\mathcal{N}}v_h(W_1) + R_{\mathcal{N}}v_h(W_2)). \quad (\text{A.6})$$

This immediately implies that the maximum and the minimum values of  $R_{\mathcal{N}}v_h(V)$  in  $\mathcal{V}(\mathcal{S}_h, e)$  are attained at the endpoints  $V_e^1$  and  $V_e^2$ , and that for any  $V$  and  $W$  in  $\mathcal{V}(\mathcal{S}_h, e)$  we have

$$|R_{\mathcal{N}}v_h(V) - R_{\mathcal{N}}v_h(W)| \leq |R_{\mathcal{N}}v_h(V_e^1) - R_{\mathcal{N}}v_h(V_e^2)|. \quad (\text{A.7})$$

Then, for each face  $f$ , we consider its decomposition  $\mathcal{S}_h|_f$  into regular-shaped triangles (again, due to our assumption **(HG)**). Let us consider the system

$$\sum_{W \in \mathcal{V}_{(\mathcal{S}_h, f)}(V)} [R_{\mathcal{N}}v_h(V) - R_{\mathcal{N}}v_h(W)] = 0 \quad \forall V \in \mathcal{V}_0(\mathcal{S}_h, f), \quad (\text{A.8})$$

where the unknowns are clearly the values of  $R_{\mathcal{N}}v_h$  in  $\mathcal{V}_0(\mathcal{S}_h, f)$ , while the values at vertices on  $\partial f$  have been assigned already in (A.4) and (A.5). It is immediate to check that the matrix associated to the system (A.8) is an M-matrix. In particular, the system has a unique solution, and we have again the discrete maximum principle. The maximum and minimum values of  $R_{\mathcal{N}}v_h$  are attained at the vertices of  $\mathcal{V}(\mathcal{S}_h, \partial f)$ . In particular, for all vertices  $V$  and  $W$  in  $\mathcal{V}(\mathcal{S}_h, f)$ , we have

$$\left| R_{\mathcal{N}}v_h(V) - R_{\mathcal{N}}v_h(W) \right| \leq \max_{V \in \mathcal{V}(\mathcal{S}_h, \partial f)} R_{\mathcal{N}}v_h(V) - \min_{V \in \mathcal{V}(\mathcal{S}_h, \partial f)} R_{\mathcal{N}}v_h(V). \quad (\text{A.9})$$

Thanks to our assumptions on the geometry (consequence **(C1)**), this implies that

$$\left| R_{\mathcal{N}}v_h(V) - R_{\mathcal{N}}v_h(W) \right| \leq \gamma \sum_{e \in \partial f} \left| \left( \mathcal{G}\mathcal{R}\mathcal{A}\mathcal{D} v_h \right)_{|e} \right| \quad \forall V, W \in \mathcal{V}(\mathcal{S}_h, \partial f). \quad (\text{A.10})$$

Using the triangle inequality and once more the assumption **(HG)** (in particular, the fact that we have less than  $N_f$  faces in  $\partial P$ ), we easily have

$$\left| R_{\mathcal{N}}v_h(V) - R_{\mathcal{N}}v_h(W) \right| \leq \gamma \sum_{e \in \partial P} \left| \left( \mathcal{G}\mathcal{R}\mathcal{A}\mathcal{D} v_h \right)_{|e} \right| \quad \forall V, W \in \mathcal{V}(\mathcal{S}_h, \partial P). \quad (\text{A.11})$$

Finally, in each polyhedron we consider the decomposition  $\mathcal{S}_h|_P$ , and the system

$$\sum_{W \in \mathcal{V}(\mathcal{S}_h, P)(V)} \left[ R_{\mathcal{N}}v_h(V) - R_{\mathcal{N}}v_h(W) \right] = 0 \quad \forall V \in \mathcal{V}_0(\mathcal{S}_h, P), \quad (\text{A.12})$$

where the unknowns are the values of  $R_{\mathcal{N}}v_h$  in  $\mathcal{V}_0(\mathcal{S}_h, P)$  and the values at vertices of  $\mathcal{V}(\mathcal{S}_h, \partial P)$  were assigned in the previous construction. Again the system has a unique solution, and we have the discrete maximum principle as in (A.7) and (A.9): for every  $V$  and  $W$  in  $\mathcal{V}(\mathcal{S}_h, P)$

$$\left| R_{\mathcal{N}}v_h(V) - R_{\mathcal{N}}v_h(W) \right| \leq \max_{V \in \mathcal{V}(\mathcal{S}_h, \partial P)} R_{\mathcal{N}}v_h(V) - \min_{V \in \mathcal{V}(\mathcal{S}_h, \partial P)} R_{\mathcal{N}}v_h(V). \quad (\text{A.13})$$

Therefore, using (A.11), we get

$$\left| R_{\mathcal{N}}v_h(V) - R_{\mathcal{N}}v_h(W) \right| \leq \gamma \sum_{e \in \partial P} \left| \left( \mathcal{G}\mathcal{R}\mathcal{A}\mathcal{D} v_h \right)_{|e} \right| \quad \forall V, W \in \mathcal{V}(\mathcal{S}_h, P). \quad (\text{A.14})$$

At this point we defined the values of  $R_{\mathcal{N}}v_h$  at all vertices of  $\mathcal{S}_h$ . We note that (A.1) is satisfied (we actually started from it). We can now extend linearly  $R_{\mathcal{N}}v_h$  in the interior of the tetrahedra of  $\mathcal{S}_h$ , using its values at the four vertices. From (A.14) we have two easy consequences. First,

$$\|\mathbf{grad} R_{\mathcal{N}}v_h\|_{0, P}^2 \leq h_P \gamma \sum_{e \in \partial P} \left| \left( \mathcal{G}\mathcal{R}\mathcal{A}\mathcal{D} v_h \right)_{|e} \right|^2, \quad (\text{A.15})$$

which is (A.2). Second, for every vertex  $V$  in  $P$ ,

$$\|R_{\mathcal{N}}v_h - v_h(V)\|_{0, P}^2 \leq h_P^3 \gamma \sum_{e \in \partial P} \left| \left( \mathcal{G}\mathcal{R}\mathcal{A}\mathcal{D} v_h \right)_{|e} \right|^2, \quad (\text{A.16})$$

which is (A.3).

**Remark 7.2.** As we already pointed out, it is not difficult to design assumptions other than **(HG)** that will still ensure (A.1)–(A.3). In particular, the present construction mimics a conceptually simpler one: first define  $R_N v_h$  on the edges of  $\mathcal{T}_h$  by linear extension from the values at their endpoints, then take the (two dimensional) harmonic extension to each face (using the values at the edges as boundary conditions), and finally take the (three dimensional) harmonic extension to each polyhedron (using the values at the faces as boundary conditions). It is not difficult to see that, under minor regularity requirements on the geometry of each  $P$ , such a construction will produce a function in  $\mathcal{H}^1(\Omega)$  satisfying (A.1)–(A.3). For instance we could require (and this, already, would be *much more* than enough) that there exist two constants  $N_s$  and  $\rho_s$  such that: (a) each  $P$  has less than  $N_s$  faces; (b) each face  $f$  has less than  $N_s$  edges; (c) each  $f$  is star-shaped with respect to all points of a disk of radius  $\rho_s h_P$ ; and (d) each  $P$  is star-shaped with respect to all points of a sphere of radius  $\rho_s h_P$ . The present setting, however, has the merit of requiring no background on the regularity of harmonic functions in corner domains [10].

*Acknowledgements.* The work of the third author was carried out under the auspices of the National Nuclear Security Administration of the US Department of Energy at Los Alamos National Laboratory under Contract No. DE-AC52-06NA25396 and the DOE Office of Science Advanced Scientific Computing Research (ASCR) Program in Applied Mathematics Research. The work of the first two authors has been partially funded by the Italian PRIN project No. 2006013187.

The authors thanks Dr. Gao Garimella (LANL) for his help in generating polyhedral meshes.

## REFERENCES

- [1] P.B. Bochev and J.M. Hyman, Principles of mimetic discretizations of differential operators, *IMA Hot Topics Workshop on Compatible Spatial Discretizations* **142**, D. Arnold, P. Bochev, R. Lehoucq, R. Nicolaides and M. Shashkov Eds., Springer-Verlag (2006).
- [2] S. Brenner and L. Scott, *The mathematical theory of finite element methods*. Springer-Verlag, Berlin/Heidelberg (1994).
- [3] F. Brezzi and A. Buffa, *General framework for cochain approximations of differential forms*. Technical report, Istituto di Matematica Applicata e Technologie Informatiche (in preparation).
- [4] F. Brezzi, K. Lipnikov and M. Shashkov, Convergence of mimetic finite difference method for diffusion problems on polyhedral meshes. *SIAM J. Numer. Anal.* **43** (2005) 1872–1896.
- [5] F. Brezzi, K. Lipnikov and V. Simoncini, A family of mimetic finite difference methods on polygonal and polyhedral meshes. *Math. Mod. Meth. Appl. Sci.* **15** (2005) 1533–1552.
- [6] F. Brezzi, K. Lipnikov and M. Shashkov, Convergence of mimetic finite difference method for diffusion problems on polyhedral meshes with curved faces. *Math. Mod. Meth. Appl. Sci.* **16** (2006) 275–297.
- [7] F. Brezzi, K. Lipnikov, M. Shashkov and V. Simoncini, A new discretization methodology for diffusion problems on generalized polyhedral meshes. *Comput. Methods Appl. Mech. Engrg.* **196** (2007) 3692–3692.
- [8] J. Campbell and M. Shashkov, A tensor artificial viscosity using a mimetic finite difference algorithm. *J. Comput. Phys.* **172** (2001) 739–765.
- [9] P.G. Ciarlet, *The finite element method for elliptic problems*. North-Holland, New York (1978).
- [10] M. Dauge, *Elliptic boundary value problems on corner domains: smoothness and asymptotics of solutions*. Springer-Verlag, Berlin, New York (1988).
- [11] P. Dvorak, New element lops time off CFD simulations. *Mashine Design* **78** (2006) 154–155.
- [12] S.L. Lyons, R.R. Parashkevov and X.H. Wu, A family of  $H^1$ -conforming finite element spaces for calculations on 3D grids with pinch-outs. *Numer. Linear Algebra Appl.* **13** (2006) 789–799.
- [13] L. Margolin, M. Shashkov and P. Smolarkiewicz, A discrete operator calculus for finite difference approximations. *Comput. Meth. Appl. Mech. Engrg.* **187** (2000) 365–383.
- [14] P.A. Raviart and J.-M. Thomas, A mixed finite element method for second order elliptic problems, in *Mathematical Aspects of the Finite Element Method*, I. Galligani and E. Magenes Eds., Springer-Verlag, Berlin-Heilderberg-New York (1977) 292–315.